Brake Pedal Displacement Measuring System based on Machine Vision

Wang Chang, Qin Jiahe, and Guo Minghua
Chang'an University / School of Automobile, Xi'an, China
Email: xawangchang@yeah.net

***Abstract*—Displacement of brake pedal was an important characteristic of driving behavior. This paper proposed a displacement measure algorithm based on machine vision. Image of brake pedal was captured by camera from left side, and images were processed in industry computer. Firstly, average smooth algorithm and wavelet transform algorithm were used to smooth the original image consecutively. Then, edge extracting method which combined Roberts's operator with wavelet analysis was used to identify the edge of brake pedal. At last, least square method was adopted to recognize the characteristic line of brake pedal's displacement. The experimental results demonstrated that the proposed method takes the advantages of Roberts's operator and wavelet transform, it can obtain better measurement result as well as linear displacement sensors.**

***Index Terms*—Displacement of Brake Pedal, Machine Vision, Edge Extraction, Wavelet Transform, Least Square Method**

I. INTRODUCTION

Transport safety was influenced by driving behavior directly. In order to research the diving behavior during driving process, some kinds of sensors were needed to capture the characterization parameters of driving behavior [1], then the researchers can get the mathematical models of driving behaviors and these models can be used in the filed of Intelligent Transportation System(ITS) [2] , such as automotive driving of vehicles [3]. During the driving process, drivers operated accelerate pedal [4], brake pedal, clutch pedal frequently. The operation of brake pedal was a typical characterization of driving behavior [5], in order to research the driver's operation of brake pedal, linear displacement sensor or force sensor for brake pedal were used in the test of driving behavior to capture the action of driver's foot. But the using of linear displacement sensor will cause interference for diver's normal operation, and the force sensor can lead to losing force feedback of brake pedal. So, how to measure the displacement of brake pedal during natural driving process was a key problem for the research of safety driving [6].

With the development of machine vision recent years, non-contact measure systems based on machine vision were used in many fields for these systems had the advantages of non-interference, fast rate, and high accuracy. Wang Da [7] proposed an image analysis algorithm based on neural networks, and it realized accurately identification of different cloud images. Huang Yingping [8] et al described an advanced testing system, combining model-based testing and machine vision technologies with the aim of automated vehicle design validation, and the experiments demonstrated that the system developed was accurate for measuring the pointer position, bar graph position, pointer angular velocity, and indicator flash rate. Fravolini Mario Luca et al [9] designed a semi-autonomous aerial refueling system based on machine vision. Takanashi Tetsuya [10] used color image segmentation technology to realize object detection from images, and the region growing algorithm, RGB color model improved the detect accuracy. Besides, image processing method can be used in different conditions for its advantage of non-contact measurement [11], high process frequency, and low cost. In order to realize the measurement of brake pedal displacement for the vehicles that equipped with automatic transmission, a brake pedal displacement measure system based image processing was designed and realized in this paper. By using this system, the normal operation of drivers will not be interfered, and this system can realize continues measurement for brake pedal displacement. Camera that installed in the left side of brake pedal capture images of brake pedal, then these images were processed in computers in order to distinguish the position of brake pedal in image, and displacement of brake pedal can be calculated from the position of brake pedal [12].

II. HARDWARE SYSTEM

A. System Structure

The system structure of brake pedal displacement system was showed as Fig. 1; this system contained IEEE 1394 industry camera, pentax H1214-M lens, 1394 image capture card and industry computer. LED ring light source was adopted for the ray in place where brake pedal installed was dark always, so the using of LED ring light source can improved the image contrast, and this was beneficial for the processing of brake pedal images later. Images captured by cameras were transmitted to computer by IEEE 1394 image capture card.

B. Industry Camera

IEEE1394 interface industry camera was used in this syste. Considering the measuring accuracy was decided by the image process, the resolution of cameras should be

doi:10.4304/jmm.8.5.632-638

high and the stability of cameras also should be fine. In order to satisfy these requirements, the displacement measure system chose the BASLER scA1000-20 IEEE1394 interface monochrome digital camera. The camera was connected to computer by IEEE 1394 image capture card and the maximum transmit rate can achieve 800 Mbps, and it can satisfy the requirement of transmit rate. BASLER scA1000-20 camera used 1/3" SONY CCD chip and its resolution was 1034×779, the maximum frame rate of this camera can be set to 20 frames per second. The camera lens that used for scA1000-20 was pentax H1214-M and this lens was attached to camera by C interface.

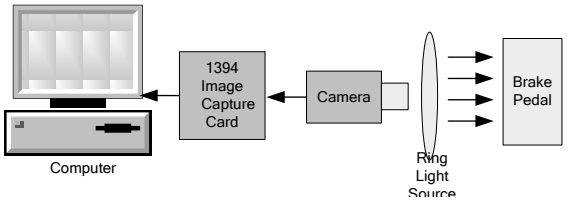

Figure 1. System structure.

Camera was installed in left side of brake pedal and the lens was installed towards the brake pedal. The size and position of brake pedals were variable for different type vehicles, thus the position of camera should be suitable with the changing of vehicle type. The installation principle for camera position was that once the brake pedal in condition of no-load, the brake pedal should in the upper right corner near the center point of image; and when the brake pedal in condition of full-load, the brake pedal should not offset out of the image.

C. Light Source

The ray in place where camera installed was dark and it changed frequently according to the variable of environment ray, and this will increasing the difficulty of image processing. In order to improve the illumination condition for camera that captured the images of brake pedal, ring LED light source was chose to improve the shading level of brake pedal. Ring LED light source was installed coaxially with the lens, and the light source consisted several white LED. This ring LED light source had the advantage of balanced brightness, and there were no flicker or shadow in ray, thus the brake pedal in the images was clearly. Further more, the brightness of areas besides brake pedal was balanced, and there were no obvious disturbing objects in these areas, all of this were helpful for the image processing program to calculate the displacement of brake pedal.

III. IMAGE PROCESSING ALGORITHM

Images of brake pedal which captured by camera will be processed by image processing program, and then the shape of brake pedal can be gained. By using the method that combined wavelet transform and Hough transform, equation of brake pedal characteristic line in the shape images of brake pedal can be extracted. Compared this equation with the equation when the brake pedal was in no-load state, the displacement of brake pedal can be calculated from these two equations.

The image processing program was compiled in Visual C++ 2010, and the image process frequency was set as 20Hz. After every process for an image, the measuring time and displacement of brake pedal calculated by image processing program were saved into the data file, which was in the format of EXCEL 2007. The specific of image processing was list as follows:

A. Wavelet Transform

Fourier transform was widely applied in engineering field for its intuitiveness, mathematical perfection, and validity of the calculation. But Fourier transform was integral on the whole time axis and it represents the global features of the target signal. In this way, Fourier transform was not suitable to analyze the partial feature of original signal. However, wavelet transform was a powerful analysis tools in time-frequency signal processing field, and it was developed by overcoming the disadvantage of Fourier transform. Nowadays, Wavelet transform has been used in many fields successfully, such as signal processing, image processing, pattern recognition, and others. Wavelet transform had good performance both in time field and frequency field; it can provide the frequency information of each frequency sub segment of target signal, which was very useful for signal classification. Wavelet transform can transform a signal into several wavelet series. So, signals can be depicted by wavelet coefficient accurately. Generating wavelet function $\psi(t)$ will be performed scaling and offsetting [13]. The stretch factor was *a* and shift factor was τ, then,

$$\psi_{a,\tau}(t) = a^{\frac{1}{2}}\psi\left(\frac{t-\tau}{a}\right), a > 0, \tau \in R. \qquad (1)$$

The function $\psi_{a,\tau}(t)$ which based on the parameters *a* and τ, was taken as wavelet basis function. If the signal was decomposed in this function system, it can get continuous wavelet transform. The decomposition of the original signal can be represented as following.

$$x(t) = \sum_k \sum_j d_{j,k} \cdot \psi_{j,k}(t). \qquad (2)$$

where $d_{j,k}$ wavelet expansion coefficient, j and k were all positive integers. The steps of wavelet transform were shown as below:

Step 1: The wavelet function $\psi(t)$ was compared with the beginning part of the original signal $f(t)$.

Step 2: Calculation of coefficient *c*. This coefficient represents the approximation between wavelet function and the original signal. The higher the value of the coefficient *c* was, the signal and wavelet will be more similarly. So, coefficient c can reflect the relevant.

Step 3: If the wavelet was offset to the right, represent the distance between the wavelet and original signal with parameter k, then the new wavelet function will be established as $\psi(t-k)$. After that, step one and step two will be repeated, and the wavelet was continuously offset

towards right, so it can be obtained wavelet function $\psi(t-2k)$. Those above process will be carrying out until the signal $f(t)$ was finished.

Step 4: The wavelet $\psi(t)$ will be extended, such as extended twice and the wavelet function was $\psi(t/2)$.

Step 5: Repeat step 1 ~ 4. The specific process was as shown in Fig. 2.

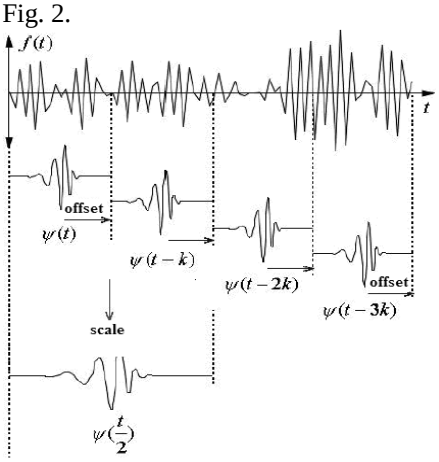

Figure 2. Flow charts of wavelet transform.

B. Image Smooth

Images captured by camera were affected by environment conditions like ray, backdrop and slight librations, thus there were some noise interference existed in images. These noise points had a common feature that all of this points were separated from the image areas of brake pedal, accelerate pedal or driver's foot. In order to wipe off these points, smoothing filtering based on wavelet analysis was adopted in image processing program.

Firstly, the smoothing filtering process using 3×3 pixels as smooth matrix. The gray level of middle pixel A was replaced by the average pixel gray level of 8 pixels around A. By gliding the smooth matrix traversal of one frame image, it will improve the quality of the vision of brake pedal.

Secondly, while carrying out multi-scale wavelet transform for images, set the scale factor as J, and then it can get $3\times J+1$ pictures. These images can be specifically represented as following.

$$c_J, \{d_j^1, d_j^2, d_j^3\}, j = 1, 2, ...J. \quad (3)$$

where c_J was the low frequency sub-band image after two-dimensional wavelet transform for the original image. d_j^k was a high frequency detail sub-band image and $d_j^1, d_j^2, d_j^3 (j = 1, 2, 3)$ were the corresponding high frequency sub-band image horizontal component, vertical part, and diagonal part correspondingly.

In order to obtain the precise image contour, after the steps above, wavelet analysis will be used to wipe off the noise segments in brake pedal image. The basic idea of wavelet denoising can be summarized as follow: the signals include noise were decomposed into multi-scale and wavelet transform will be carried out in binary type. The wavelet coefficient belong to the noise will be removed from the original signal, and the wavelet coefficient which belong to the useful signal will be enhanced. In different resolution, the wavelet coefficients of signal present can be variable. By setting and adjusting the threshold of wavelet coefficients can improve the de-noising quality. By using this image smooth method, original image of brake pedal will be converted as Fig. 3.

(a) Original image

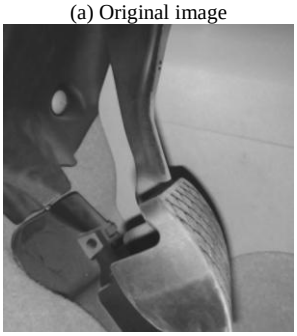

(b) Smoothed image

Figure 3. Flow charts of wavelet transform.

C. Image Enhancement and Binarization

Image enhancement can improved the edge characteristic of brake pedal image, and the accuracy of displacement measuring can be increased. Histogram equalization method was used in the image process program to enhance the image with the result of Fig. 4.

Figure 4. Image after enhancement.

Image binarization can reduce the complex level of images, and the time that the program spent on extracting shape of brake pedal can be reduced largely, thus the image processing rate can be improved. All pixels in a frame image will be carrying out binary processing, if a pixel's gray level was greater than threshold value, then this pixel value was converted to 0, otherwise it will be

converted to 1. The difficulty of binary process was the determination of gray threshold because gray threshold should be variable in different illumination conditions. The image processing program adopted adaptive threshold to carry out binary as follows [14]:

Step 1: Calculated the summation of gray level for a frame image and the average of gray level Q will be got.

$$Q = \frac{\sum_{i=0}^{m-1}\sum_{j=0}^{n-1} x_{ij}}{m \times n}. \quad (4)$$

Step 2: Set the gray threshold K=1.25×Q, carried out binary with K for images and other processing steps.

Step 3: Carried out following steps of image processing to extract shape image of brake pedal. If the result of extracting shape image of brake pedal was abnormal, this meant the gray threshold was unsuitable at this time; it should be recalculated by the above-mentioned two steps. The following steps of image processing will adopted new gray threshold.

Test experiments results showed that the method of adaptive threshold had good stability, and gray threshold can keeping stable in places where ray changed little and it can changing the threshold automatically once the rays changed greatly. This method of adaptive threshold can guaranteed the normal running of system [15]. Fig. 5 was the pedal image after binarization.

Figure 5. Image after binarization.

D. Shape Extraction of Brake Pedal

The shape extraction of brake pedal was carried out by using edge extraction algorithm. Roberts's operator, Prewitt operator, Sobel operator and Laplacian operator were used widely to carry out edge extraction. The accuracy and inhibition of error point of each operator were different. In order to improve the accuracy of edge extraction, image processing program adopted Roberts's operator and wavelet transform to carry out edge extraction. Roberts operator had the advantage of high accuracy, but it was sensitive to error points, so the Roberts operator was usually used for images that had clear edge and little error points. The image quality of brake pedal was improved and there were little error points in image because the LED light source illuminated the brake pedal uniformly. After the smooth step, the brake pedal's edge was clear and there were little error points in image, so it's appropriate to use Roberts operator to extract edge of brake pedal.

$$|\nabla f(x,y)| = \sqrt{(f(x,y)-f(x+1,y+1))^2+(f(x+1,y)-f(x,y+1))^2} \quad (5)$$

Template matrix was used to carry out edge extraction in real image processing, convert (5) to template matrix as

$$\begin{bmatrix} 1 & 0 \\ 0 & -1 \end{bmatrix}\begin{bmatrix} 0 & 1 \\ -1 & 0 \end{bmatrix}. \quad (6)$$

Firstly, for a frame of binary image, using the above template matrix to extract edge from the first row to the final row and from the first column to the final column, then the edge basic area of brake pedal will be gained once all pixels were calculated by template matrix. As Fig. 5 shows, there were other characteristic line that not belong to break pedal, so the Roberts operator can recognize all of the line in images, but it can determined which line was the characteristic line of brae pedal. Aiming at this problem, wavelet transform will be used to extract characteristic line of brake pedal.

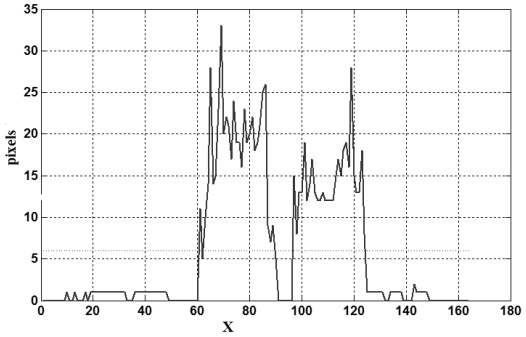

(a) Feature area on X-axis

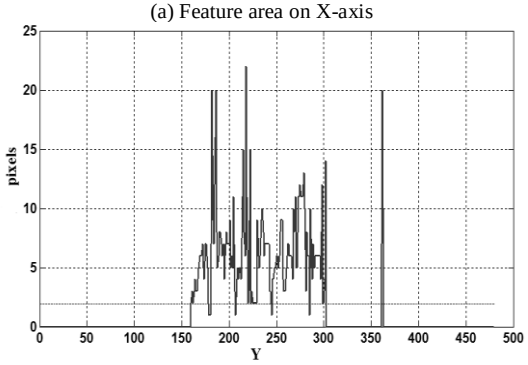

(b) Feature area on Y-axis

Figure 6. Distribution of feature area.

The scale of wavelet transform has a certain influence on image feature extraction and large scales correspond to the low frequency characteristics of the signal, small scales correspond to the low frequency characteristics. The larger the transformation scale, the amount of calculation will be greater. In order to select the reasonable transformation scale, the appropriate transformation scale can be selected based on the distribution of the statistical characteristics after analysis on the statistical features of images. Finally, the scale factor was setting into two. The whole image not only included the target domain, but also included the background domain. In generally, the identified goal was

a connected domain in which the gray value not had distortion. The gray boundary between the target domain and the non-target domain will change. Thus, according to the local boundary gray gradient change, it can't locate the target area accurately. After the statistics of boundary pixels, distribution of pixels was adopted to determine the position of the target domain [16]. Fig. 6 shows the distribution of the target domain pixels.

Fig. 6 shows the distribution of the logic coordinates X in the target domain presents bimodal characteristics, and the range was from 0 to 120. It indicated the target domain presents strip distribution along Y axis which is consistent with the result of wavelet edge detection. Coordinate Y mainly distributed between 150 and 300, and it shows certain volatility.

By carrying out J scales two-dimensional wavelet transform, detail coefficients of each decomposition level can be obtain. Each decomposition level included the detail coefficients of horizontal, vertical and diagonal part, as well as the approximate coefficient of the top level. Its result is shown as follow:

$$\{e_j^1, e_j^2, e_j^3\}, j = 1, 2, ...J . \tag{7}$$

$e_j^k = \text{mean2}(d_j^k)$ was the mean of the corresponding sub-band image. The statistical feature vector indicates the image energy distribution in different scales and different directions; it included the identified valuable attributes in image mode. Here, each image will performed two scale two-dimensional wavelet decomposition and forming a statistical characteristic vector including seven elements. Finally, the vector *F(p)* was:

$$F(p) = [427.2136, -0.2876, 0.3814, 0.0900, -0.0040, -0.2315, -0.0063]$$

Once statistical characteristic vector extracted from the image, the similarity between them can be calculated. F(p) and F(q) were two image statistical characteristic vectors. The cosine of the angle ϕ between statistical characteristic will be used to represent the similarity between statistical characteristic and the value of ϕ was in the range from 0 to π.

$$R_v(p,q) = \cos\phi = \frac{|F(p) \times F(q)|}{|F(p)| \times |F(q)|} . \tag{8}$$

Finally, after feature extraction and image matching, and finally the results was showed in Fig. 7.

E. Linear Fitting of Brake Pedal

The left upper edge of brake pedal was used as characteristic line which will be used to calculate the displacement of brake pedal. Once the characteristic line of brake pedal was obtained, comparing the line with the characteristic line when the brake pedal was in no-load state, then the angle θ between these two lines can be calculated from equations of these two lines. By using method of linear fitting, the line equation of characteristic line at any time can be calculated.

Fig. 7 shows that there were not only lines existed in image, but also arcs, points and so on. If used the least squares method to carry out linear fitting directly, the un-linear area should be eliminated firstly, but this process needed more time and the accuracy of linear fitting was poor. At now, Hough transform was used to extract line area in image widely. The noise suppression of Hough transform was good, but the accuracy was difficult to control. Considering the characteristic of least squares and Hough transform, and in order to improve the accuracy of line extraction, this system used a method combined Hough transform and least squares to extraction line area in the image of brake pedal. The specific of line extraction was list as follow:

1. Hough transforms. For a certain time of measuring i, using Hough transform to extract line area and convert the line equation into normal form as (9) and calculated the parameters a_i, b_i of line equation. It's necessary to select the characteristic line equation of brake pedal for the number of lines that extracted by Hough transform always more than one. The selecting method adopted the line length and the line slope a_i to confirm which line was the characteristic line because the length of brake pedal was fixed, and the turning angle of brake pedal was also limited in a certain range [17].

$$y = a_i x + b_i . \tag{9}$$

2. Distance judgment. For an arbitrary point A (x_A, y_A) which was got from Hough transform, calculate the distance d_A of point A to line L and the distance d_B of point B (x_B, y_B) to line L which was near by point A. If $d_B < d_A$, it means that the point B was also belonging to line L, but the Hough transform did not extracted this point. Added the point B to the point set M of line L. If $d_B \geq d_A$, it means that the point B was not belonging to line L, so this point will be abandoned. Calculated all points of line L, added the suitable points to point set, and then a new point set M′ of line L will be formed.

3. Linear fitting of least squares. For points in the new point set M′, according to the least square method, linear fitting for characteristic line equation of brake pedal will be carried out, and the parameters a', b' of new characteristic line L′ was calculated as

$$a' = \frac{\sum x_i y_i \sum x_i - \sum y_i \sum x_i^2}{(\sum x_i)^2 - n\sum x_i^2}$$
$$b' = \frac{\sum x_i \sum y_i - n\sum x_i y_i}{(\sum x_i)^2 - n\sum x_i^2} . \tag{10}$$

F. Calculation of Displacement

Characteristic parameters of brake pedal should be confirmed firstly. Line distance from a certain measure place to the place in no-load condition was used as characteristic parameters of brake pedal generally. Considering the structure of brake pedal, it was more accurate to use the turning angle θ of brake pedal than linear displacement for during the process of working, brake pedal turning around with a fixed point all the time.

In this system, the angle θ between the process of brake pedal and no-load state was adopted as the Characteristic parameter of brake pedal. By multiplying the angle θ with the turning radius of brake pedal, the linear displacement will be got and it was more accuracy than other methods.

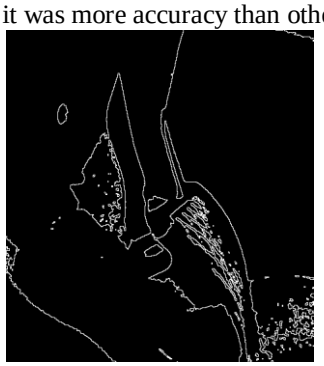

Figure 7. Result of edge extraction.

The characteristic line L′ was obtained by linear fitting. The line equation $y_0 = a_0 x + b_0$ of brake pedal in no-load state should be calculated firstly. For a certain time of measurement, the equation of line L′ was $y_i = a_i x + b_i$. By using the angle calculating equation between two lines in a plane, the angle θ between line y_i and y_0 was calculated as

$$\theta = \arctan\left|\frac{a_i - a_0}{1 + a_i a_0}\right|. \tag{11}$$

IV. Measuring Accuracy Validate

Installed and debugged this brake pedal displacement measuring system in test vehicle. In order to validate the accuracy of this system, kubler D8.3A linear displacement sensor was installed in test vehicle at the same time. The accuracy of kubler D8.3A was 0.1%. Sampled displacement of brake pedal in different vehicle running conditions used parameter angle θ of image system and parameter line distance L of kubler D8.3A system.

For angle θ from image processing, using the trigonometric function to calculate linear displacement of brake pedal as

$$L = 2R \sin\frac{\theta}{2} \tag{12}$$

R was the radius of brake pedal turning, θ was the angle from image processing. Verifying test result was showed in Fig. 8.

Comparing the linear displacement calculated from image processing with linear displacement from D8.3A sensor at the same time, the results showed that the error of linear displacement from image processing was less than 2mm. In most time of measurement, the relative error was small and results of repeated measurement kept stable. Comparing with D8.3A linear sensor, the accuracy of image processing to calculate displacement was lower, but this method did not need any refit for brake pedal, and the normal operation of driver will not be disturbed by this system. On the other hand, this system was designed to using in the test field of driving behavior. The accuracy requirement of driving behavior test was lower than the vehicle control and stability test, the real using result showed that error of 2mm can satisfy the requirement of driving behavior test.

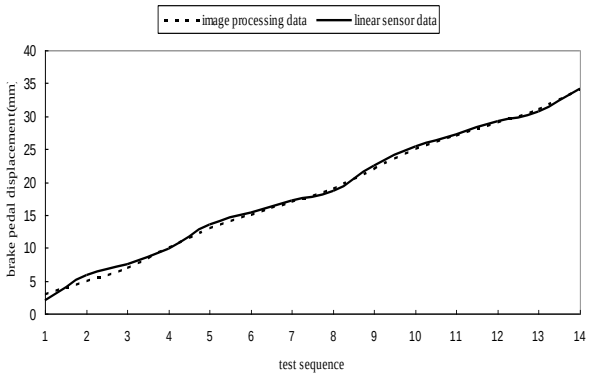

Figure 8. Result of verifying experiments.

V. Conclusion

The real time measurement of brake pedal displacement was realized by using of machine vision. Processing the image captured by camera installed in left side of brake pedal with smoothing filtering, image binary, edge extraction and Hough transform. Combining the method of least squares linear fitting, brake pedal turning angle was calculated. Then the linear displacement of brake pedal can be calculated from turning angle and radius. This system did not need any refit for brake pedal and the normal operation of driver will not be disturbed. Results of plenty of real test showed that this system had the advantage of high accuracy, fast rate and better stability. For the structure of different vehicles, this system was limited to use only for vehicles which equipment with automatic.

Acknowledgment

This work was supported in part by a grant from Program for Changjiang Scholars and Innovative Research Team in University (IRT1286) and National Natural Science Foundation of China (51178053).

References

[1] B. B. Zhu, M. D. Swanson, and A. H. Tewfik, “When seeing doesn’t believe,” *IEEE Signal Processing Magazine*, vol. 21, pp. 40–49, March 2004.

[2] S. S. Wang, S. L. Tsai, “Automatic image authentication and recovery using fractal code embedding and image inpainting,” *Pattern Recognition*, vol. 41, pp. 701-712, February 2008.

[3] M. Holliman, N. Memon, “Counterfeiting attacks on Oblivious block-wise independent invisible watermarking schemes,” *IEEE Transaction on Image Processing*, vol. 9, pp. 432–441, March 2000.

[4] Rastislav Lukac, Konstantinos N. Plataniotis, “Bit-level based secret sharing for image encryption,” *Pattern Recognition*, vol. 38, pp. 767–772, May 2005.

[5] Chang-Chou Lin, Wen-Hsiang Tsai, "Secret image sharing with steganography and authentication," *journal system and software*, vol. 73, pp. 405–414, December 2004.
[6] D. S. Tsai, G. Horng, T. H. Chen, and Y. T. Huang, "A novel secret image sharing scheme for true-color images with size constraint," *Journal of Information Science*, vol. 179, pp. 3247-3257, September 2009.
[7] Wang Da, Bi Shuo-Ben, and Wang Bi-Qiang, "Cloud image iusion based on regional feature of RLNSW-NSCT and PCNN," *International Journal of Digital Content Technology and its Applications*, vol. 6, pp. 400-411, November 2012.
[8] Huang, Yingping, Mouzakitis, Alexandros, McMurran, R, Dhadyalla, G and Jones, R.P, "Design validation testing of vehicle instrument cluster using machine vision and hardware-in-the-loop", *International Conference on Vehicular Electronics and Safety*. pp. 265-270, September 2008.
[9] Mario Luca Fravolini, Giampiero Campa, and Marcello R. Napolitano, "Modelling and performance analysis of a machine vision-based semi-autonomous aerial refuelling," *International Journal of Modeling, Identification and Control*, vol.3, pp. 357-367, September 2008.
[10] Takanashi Tetsuya, Shin Jungpi, "Color image segmentation based on region growing algorithm," *Journal of Convergence Information Technology*, vol. 7, pp. 152-160, August 2012.
[11] Wang Chien-Chih, Jiang Bernard C, and Chou Yueh-Shia, "Multivariate analysis-based image enhancement model for machine vision inspection," *International Journal of Production Research*, vol. 49, pp. 2999-3021, May 2011.
[12] Zhenghao SHI, Lifeng He, "Current status and future potential of neural networks used for medical image processing," *Journal of Multimedia*, vol. 6, pp. 244-251, June 2011.
[13] Server Kasap, Khaled Benkrid, "Parallel processor design and implementation for molecular dynamics simulations on a FPGA-based supercomputer," *Journal of Computers*, vol. 7, pp. 1312-1328, June 2012.
[14] Jinliang Wan, Yanhui Liu, "Multi-regions texture substitution," *Journal of Multimedia*, vol. 7, pp. 394-400, December 2012.
[15] Wang Chenglong, Li Xiaoyu, and Wang Wei, "Recognition of worm-eaten chestnuts based on machine vision," *Mathematical and Computer Modelling*, vol. 54, pp. 888-894, August 2011.
[16] Qian Zhang, "Reconstruction of intermediate view based on depth map enhancement," *Journal of Multimedia*, vol. 7, pp. 415-419, December 2012.
[17] Yinpu Zhang, "Study on airspace covert communication algorithm of covert communication system," *Journal of Networks*, vol. 7, pp. 730-737, April 2012.